Monitoring statistics of the ERS-2 scatterometer for ESA

CYCLE 81

(Project Ref. 15988/02/I-LG)

Hans Hersbach
European Centre for Medium-Range Weather Forecasts,
Shinfield Park, Reading, RG2 9AX, England
Tel: (+44 118) 9499476, e-mail: dal@ecmwf.int

February 21, 2003

1 Introduction

From 12 December 2001 onwards, ESRIN redistributes ERS-2 scatterometer data to a selected group of users. The quality of this experimental gyroless product was monitored at ECMWF for cycle 81. The gyroless ERS-2 scatterometer data was not used in the 4D-Var data assimilation system at ECMWF.

Since 06 UTC 4 February 2003, a new processor, ESACA, was introduced. It is an upgrade of the existing LRDPF and includes new scatterometer processing algorithms that anticipate errors in the satellites yaw attitude control. It was installed at Kiruna station only, and is planned to run for a test period of three weeks. Only data from this station was disseminated, and as a result, for each day since 4 February 2003, no data was received between approximately 21 UTC and 06 UTC.

Because of the introduction of the new processor, some sections in this report will be split in two, elucidating the quality and characteristics of the 'old' and 'new' data.

The information content of the Missing Packet Counter (BUFR code identifier 21195) was changed for the new processor. Its absolute values are now larger, and, as a result, the usual standard Quality Control check for rejection if it is larger than 10, would apply to all 'new' data. Therefore, this check was removed from the monitoring software; both for old and newly processed data. The impact on monitoring results for data obtained with the old processor was found to be negligible for sigma0 backscatter levels, within 1% for cone distances and within 1 cm/s in wind-speed biases and standard deviations.

During cycle 81, data was received between 21:02 UTC 13 January 2003 and

20:59 UTC 17 February 2003. Besides the data gaps indicated above, no data was received during the 6-hourly periods of 18 UTC 15 January 2003 and 00 UTC 16 January 2003, between 00 UTC 18 January 2003 and 06 UTC 19 January 2003, between 12 UTC 25 January 2003 and 00 UTC 26 January 2003, and between 18 UTC 31 January 2003 and 00 UTC 01 February 2003.

Less than 25% of the normal amount of data was received during the 6-hourly periods centered around 18 UTC 17 January 2003 and 06 UTC 25 January 2003, both representing the starting point of a period without data.

The average quality of the old processed data for cycle 81 was comparable to the average performance of the data received during cycle 80. Although the negative bias in wind speed was slightly worse, the standard deviation between the UWI winds and collocated ECMWF first-guess (FGAT) winds was smaller. In addition, the number of light UWI winds collocated with much stronger FGAT winds was lower than it was for cycle 80.

The standard deviation of the UWI wind speeds determined with the new processor are also comparable to that of the winds received during cycle 80. Despite the enhanced solar activity encountered during cycle 81, there are hardly any collocations of light UWI winds with strong FGAT winds left. Also, the frequency of incorrectly de-aliased winds has been reduced drastically. Both must be attributed to the merits of ESACA.

However, it was found that the 'new' winds differ from winds inverted at ECMWF using CMOD4, which didn't use to be the case. These latter winds appear to be of much higher quality. Random error of these CMOD4 winds w.r.t. FGAT winds is 0.12 m/s lower than it is for the UWI winds. This indicates a flaw in ESACA, which can be repaired. Winds inverted on the basis of CMOD5 give best results, both in terms of bias and standard deviation.

Apart from the several interruptions of the data flow, and despite the encountered enhanced solar activity, the situation was reasonably stable during cycle 81. Time series of the normalized distance to the cone and of UWI winds minus FGAT winds showed for the 'old' data two peaks that were not related to low-data volumes. These peaks were associated with larger than normal negative wind biases, which is an indication of a yaw attitude error exceeding 2 degrees. For the 'new' data most such peaks seemed to be related to low data volumes. Other peaks seemed to be related to large values of the asymmetry between the incidence angles of the fore and aft beam. A phenomenon that emerged from the start of the ESACA period.

On 14 January 2003, a new version of the ECMWF assimilation and forecast system was introduced. The 4D-Var minimizations are now multi-incremental (T95/T159), using a new (conjugate gradient) minimization technique which requires a strictly quadratic cost function. In addition, the estimation of background statistics was improved. New data types now being assimilated are GOES water vapour radiances, MODIS winds, more HIRS channels, and ERS-2 SAR ocean wave data. SSM/I radiances are now directly assimilated, rather than their derived meteorological quantities (such as surface wind speed). Changes of the forecast system include improved cloud scheme numerics, revised cloud physics, and revised convection. As a result the quality of the ECMWF surface winds was slightly improved.

2 ERS-2 statistics from 14 January to 17 February 2003

2.1 Sigma0 bias levels

2.1.1 'Old' data: 14 January to 4 February 2003

For these data within cycle 81 the average sigma0 bias levels (compared to simulated sigma0's based on ECMWF model first-guess winds, see Figure 1) were within 0.1 dB from the corresponding levels averaged over cycle 80. For ascending tracks bias levels of the fore and mid beam have become 0.1 dB more negative at medium and high incidence angles. Bias levels of the aft beam remained the same. As a result the inter-beam agreement has improved for such tracks.

For the descending tracks there was hardly any change in bias levels.

The general picture that emerges from the ocean calibration displayed in Figure 1 is as follows. Bias levels are between 0.3 and 1.4 dB too low, gradually growing from low to high incidence angles. The inter-beam differences are within 0.3 dB, For the descending tracks, bias levels of the three beams agree very well for high incidence angles and somewhat less for low to medium incidence angles. For the ascending tracks, inter-beam differences are larger (up to 0.35 dB).

2.1.2 'New' data: 4 February to 17 February 2003

For these data within cycle 81, average sigma0 bias levels (compared to simulated sigma0's based on ECMWF model first-guess winds) are presented in Figure 2. At high incidence angles the situation has improved w.r.t. the biases encountered for the 'old' data. Bias levels are almost all less than 1 dB too low, inter-beam differences are small, and the dependency on incidence angle is milder. This latter quality is also true for the mid beam at low incidence angles. However, for the fore and aft beam bias levels are growing rapidly towards low incidence angles. the difference with the bias level of the mid beam is considerable; a clearly undesired property.

2.2 Incidence angles

By design of the ERS scatterometer instrument, the incidence angles under which the fore an aft beam illuminate the ocean surface are equal. In practice, this symmetry was achieved quite accurately. However, it was observed that for the data received during the ESACA period, both angles differ. Differences of more 9 degrees were observed. This can be seen from Figure 3, in which a time-series of the fore minus aft incidence angle is plotted. Up to the introduction of ESACA (06 UTC 4 February 2003) differences are within 0.2 degrees (archived accuracy is 0.1 degree); after the introduction, there is a rapid evolution of large differences. This large asymmetry is most likely related to inaccuracies in the satellites yaw angle.

2.3 Distance to cone history

The distance to the cone history is shown in Figure 4. During the period of the 'old' processor, two large peaks are encountered for the period between 12 UTC - 18 UTC 20 January 2003 respectively between 18 UTC 22 January and 00 UTC 23 January 2003. They are associated with peaks in the UWI wind versus FGAT time series (Figure 5; see below). They might be associated with enhanced solar activity.

During the period of the 'new' processor most the peaks appearing in the distance to cone history seem to be connected to low data volumes. However, some of them are related to a large asymmetry between the fore and aft incidence angle (Figure 3). An example is the peak at 18 UTC 8 February 2003.

2.4 UWI minus First-Guess wind history

In Figure 6, the UWI minus ECMWF first-guess wind history is plotted.

Both the wind-bias and the standard deviation history show a number of peaks, which are for 'old' data most prominent towards higher nodes, and for 'new' data strongest towards lower nodes.. Most of them also appear as peaks in the distance to the cone history. During the period of the 'old' processor, especially the peak starting at 12 UTC 20 January 2003 is associated with low quality winds. For that period of 6 hours, UWI winds compared to FGAT winds are plotted in the top panel of Figure 9. As can be seen, especially the winds at the higher nodes are far too weak, and a group of them they point in the across node direction, unrelated to the FGAT wind direction.

During the period of ESACA, the strongest peaks in relative wind bias (e.g. 00 UTC 15 February and 00 UTC 17 February 2003) are related to very low data volumes (31 resp. 191). Peaks in relative standard deviation are not induced by low data volumes, such as the peak for 18 UTC 8 February 2003. It corresponds to a peak in the fore minus aft incidence angle history (Figure 3). It is likely to be associated with a large yaw error. The coincidence of the peak in standard deviation with a peak in incidence angle differences indicates that this latter quantity might be used as a handle for quality control.

In the lower panel of Figure 9, an example of low quality UWI winds for the period of 18 UTC 8 February 2003 is shown. Winds (only for lower nodes winds were inverted) are far too low, which explains the peak in Figure 5.

In Figure 10, all locations are shown for which UWI winds were more than 8 m/s weaker than the FGAT winds. It is seen that for ESACA (lower panel) such collocations still occur, though less frequently than for the old processor during cycle 81 (top panel). The situation displayed in the lower panel of Figure 9 (near Mexico) is one of these situations. It was associated with a large asymmetry between the fore and aft incidence angle. It would be interesting to investigate whether a similar pattern could be observed for other situations displayed in the lower panel of Figure 10.

Average bias levels and standard deviations of UWI winds relative to FGAT winds are displayed in Table 1. From this it is seen that, compared to cycle 80, the bias level for 'old' data of cycle 81 has become somewhat more negative. This shift

	Cycle 80	Cycle 81			
	OLD	OLD		ESACA	
	UWI	UWI	CMOD4	UWI	CMOD4
speed STDV	1.62	1.61	1.59	1.62	1.50
node 1-2	1.60	1.57	1.55	1.57	1.53
node 3-4	1.58	1.55	1.53	1.50	1.46
node 5-7	1.57	1.55	1.54	1.54	1.43
node 8-10	1.59	1.57	1.56	1.61	1.44
node 11-14	1.63	1.62	1.61	1.63	1.46
node 15-19	1.66	1.66	1.65	1.63	1.49
speed BIAS	-1.01	-1.08	-1.11	-0.91	-0.96
node 1-2	-1.33	-1.39	-1.40	-1.59	-1.65
node 3-4	-1.19	-1.26	-1.22	-1.20	-1.21
node 5-7	-1.00	-1.08	-1.08	-0.88	-0.88
node 8-10	-0.87	-0.96	-1.00	-0.66	-0.70
node 11-14	-0.90	-0.98	-1.04	-0.61	-0.69
node 15-19	-0.97	-1.02	-1.09	-0.69	-0.77
direction STDV	49.9	50.5	18.9	28.5	19.8

Table 1: Biases and standard deviation of ERS-2 versus ECMWF FGAT winds in m/s for speed and degrees for direction

is more or less uniform as function of node number. For 'new' data during cycle 81, the overall bias has become less negative. However, the inter-node differences are enormous: from -1.59 m/s for the lowest nodes to -0.69 m/s for the highest nodes. The large negative bias at lower nodes is the result from the much too low backscatter levels of the fore and aft beam (see Figure 2).

It is seen that w.r.t. cycle 80, the standard deviation of the 'old' data for cycle 80, is very similar. This is also true for the UWI winds derived from the ESACA processor. In Table 1 results for CMOD4 winds inverted at ECMWF from backscatter triplets are shown as well. They should be almost identical to the UWI product, with the main difference that both solutions are available, which allows for de-aliasing w.r.t. the FGAT winds. This explains the differences in the standard deviation of the 'old' data for cycle 81. For the ESACA period, however, differences are very large. The CMOD4 winds have a much smaller standard deviation than the UWI winds. Apparently, the wind inversion scheme in ESACA is not optimal.

For the 'old' data of cycle 81 the (scatterometer - model) direction standard deviations were ranging between 40 and 60 degrees for the UWI data (Figure 6, for averages, see Table 1). For the ESACA data, the corresponding deviations are between 20 and 40 degrees. These values are much closer to the levels for de-aliased winds (between 15 and 25 degrees, see Figure 8). Apparently, the ESACA processor contains a much better de-aliasing algorithm.

Finally, in Figure 7, time series of the de-aliased CMOD4 versus FGAT winds are shown. It displays the drop in standard deviation (especially for the higher nodes) since the introduction of ESACA. This drop is not visible for the UWI winds

(Figure 5). Also note from Figures 5 and 7, that for the 'old' data, performance became worse after the data gap around 19 January 2003, and that it improved again after the data gap around 26 January 2003.

2.5 Scatter plots

Scatterplots of model 10 m first-guess winds versus ERS-2 winds are displayed in Figures 11 to 18. Values of standard deviations and biases are slightly different from those displayed in Table 1. Reason for this is that, for plotting purposes, the in 0.5 m/s resolution ERS-2 winds have been slightly perturbed (increases scatter with 0.02 m/s), and that zero wind-speed ERS-2 winds have been excluded (decreases scatter with about 0.05 m/s). These scatterplot elucidate the trends described in the previous section: the standard deviation of the 'old' and 'new' data of cycle 81 is comparable to that of cycle 80; and the quality of the 'new' CMOD4 winds (Figures 16 and 17) is much higher. It also shows the improved de-aliasing of ESACA (Figure 12 versus Figure 15). Although, note the strange oscillation in Figure 15. It is not present for the de-aliased CMOD4 winds (Figure 17).

Winds derived on the basis of CMOD5 are displayed in Figure 18. Both the bias level and the standard deviation is better than those for CMOD4 and UWI winds. Although CMOD5 winds are too low (induced by too low backscatter levels, see Figure 2), the random error of CMOD5 winds w.r.t. FGAT winds is lower than it has ever been for ERS-2 winds.

Figure Captions

Figure 1: Ratio of $< \sigma_0^{0.625} > / <$ CMOD4(FirstGuess)$^{0.625} >$ converted in dB for the for beam (solid line), mid beam (dashed line) and aft beam (dotted line), as a function of incidence angle for descending and ascending tracks of the 'old' data within cycle 81. The thin lines indicate the error bars on the estimated mean. First-guess winds are based on the in time closest (+3h, +6h, +9h, or +12h) T511 forecast field, and are bilinearly interpolated in space.

Figure 2: Same as Figure 1, but now for the ESACA data within cycle 81.

Figure 3: Time series of the difference in incidence angle between the fore and aft beam.

Figure 4: Mean normalized distance to the cone computed every 6 hours for nodes 1-2, 3-4, 5-7, 8-10, 11-14 and 15-19 (solid curve close to 1 when no instrumental problems are present). The dotted curve shows the number of incoming triplets in logarithmic scale (1 corresponds to 60,000 triplets) and the dashed one indicates the fraction of complete sea-located triplets rejected by the ESA flag, or by the wind inversion algorithm (0: all data kept, 1: no data kept).

Figure 5: Mean (solid line) and standard deviation (dashed line) of the wind speed difference UWI - first guess for the data retained by the quality control.

Figure 6: Same as Fig. 3, but for the wind direction difference. Statistics are computed only for wind speeds higher than 4 m/s.

Figures 7 and 8: Same as Fig. 5 and 6 respectively, but for the de-aliased CMOD4 data.

Figure 9: UWI wind vectors (red) and FGAT wind vectors (blue) within the 6-hourly period of 18 UTC 20 January 2003 south-east of South Africa (top panel) and within the 6-hourly period of 18 UTC 8 February 2003 west of Central America (lower panel).

Figure 10: Locations of data during cycle 81 (top panel old data; lower panel ESACA data) for which UWI winds are more than 8 m/s weaker than the collocated FGAT winds.

Figure 11: Two-dimensional histogram of first guess and 'old' UWI wind speeds, for the data kept by the quality control. Circles denote the mean values in the y-direction, and squares those in the x-direction.

Figure 12: Same as Fig. 11, but for wind direction. Only wind speeds higher than 4m/s are taken into account.

Figure 13: Same as Fig. 11, but for CMOD5 winds.

Figure 14 and 15: Same as Figs. 11 and 12, but for ESACA UWI winds.

Figure 16 and 17: Same as Figs. 11 and 12, but for 'new' CMOD4 winds.

Figures 18: Same as Fig. 13, but 'new' CMOD5 winds.

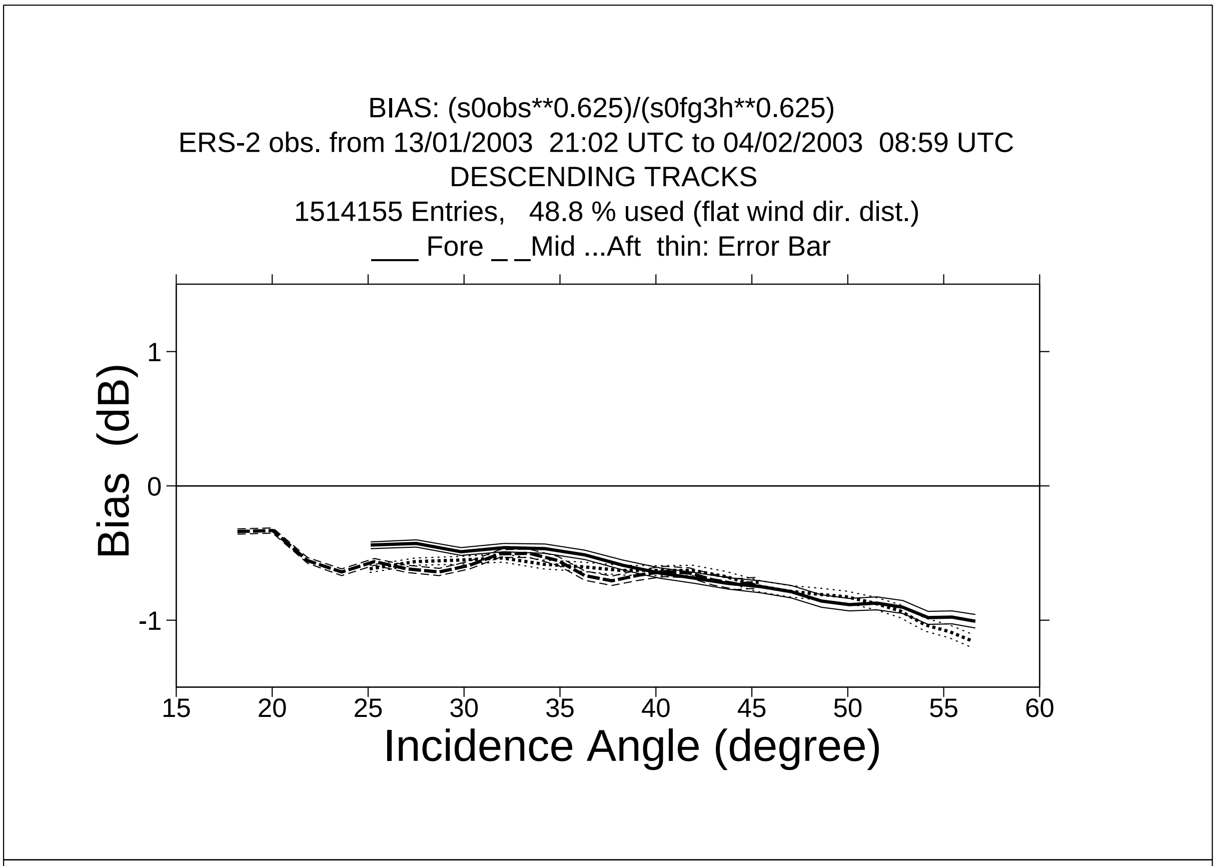
BIAS: (s0obs**0.625)/(s0fg3h**0.625)
ERS-2 obs. from 13/01/2003 21:02 UTC to 04/02/2003 08:59 UTC
DESCENDING TRACKS
1514155 Entries, 48.8 % used (flat wind dir. dist.)
___ Fore _ _Mid ...Aft thin: Error Bar
Bias (dB)
1
0
-1
15
20
25
30
35
40
45
50
55
60
Incidence Angle (degree)

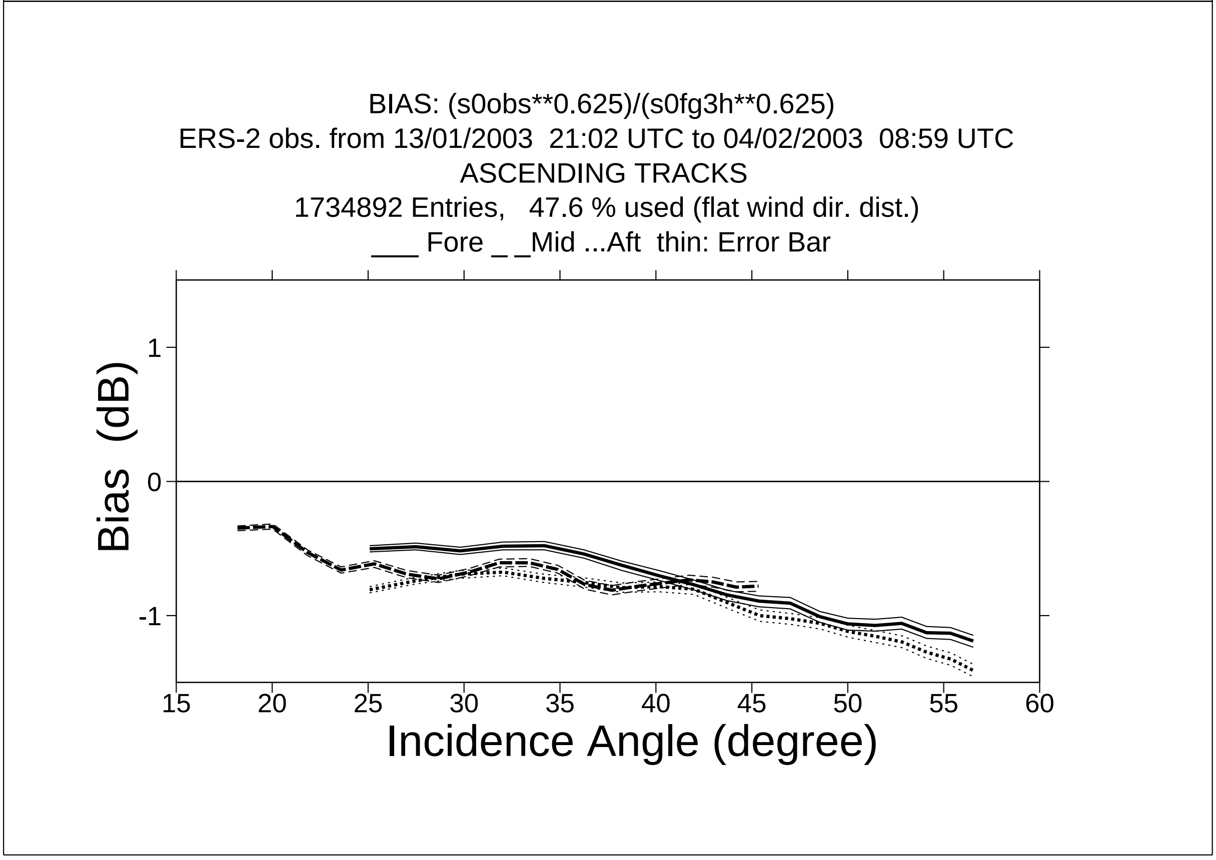
BIAS: (s0obs**0.625)/(s0fg3h**0.625)
ERS-2 obs. from 13/01/2003 21:02 UTC to 04/02/2003 08:59 UTC
ASCENDING TRACKS
1734892 Entries, 47.6 % used (flat wind dir. dist.)
___ Fore _ _Mid ...Aft thin: Error Bar
Bias (dB)
1
0
-1
15
20
25
30
35
40
45
50
55
60
Incidence Angle (degree)

Figure 1

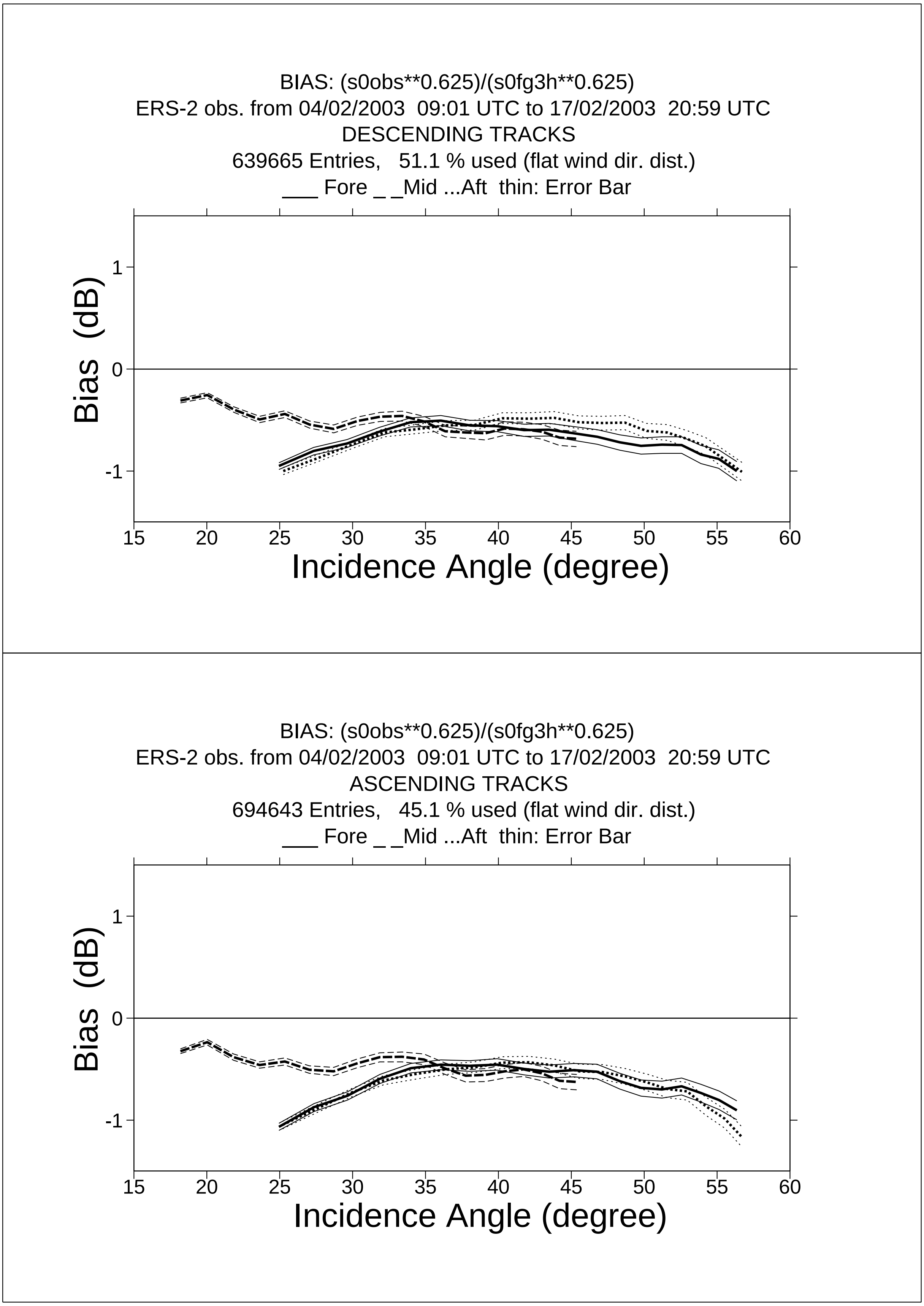
BIAS: (s0obs**0.625)/(s0fg3h**0.625)
ERS-2 obs. from 04/02/2003 09:01 UTC to 17/02/2003 20:59 UTC
DESCENDING TRACKS
639665 Entries, 51.1 % used (flat wind dir. dist.)
___ Fore _ _Mid ...Aft thin: Error Bar
Bias (dB)
1
0
-1
15
20
25
30
35
40
45
50
55
60
Incidence Angle (degree)
BIAS: (s0obs**0.625)/(s0fg3h**0.625)
ERS-2 obs. from 04/02/2003 09:01 UTC to 17/02/2003 20:59 UTC
ASCENDING TRACKS
694643 Entries, 45.1 % used (flat wind dir. dist.)
___ Fore _ _Mid ...Aft thin: Error Bar
Bias (dB)
1
0
-1
15
20
25
30
35
40
45
50
55
60
Incidence Angle (degree)

Figure 2

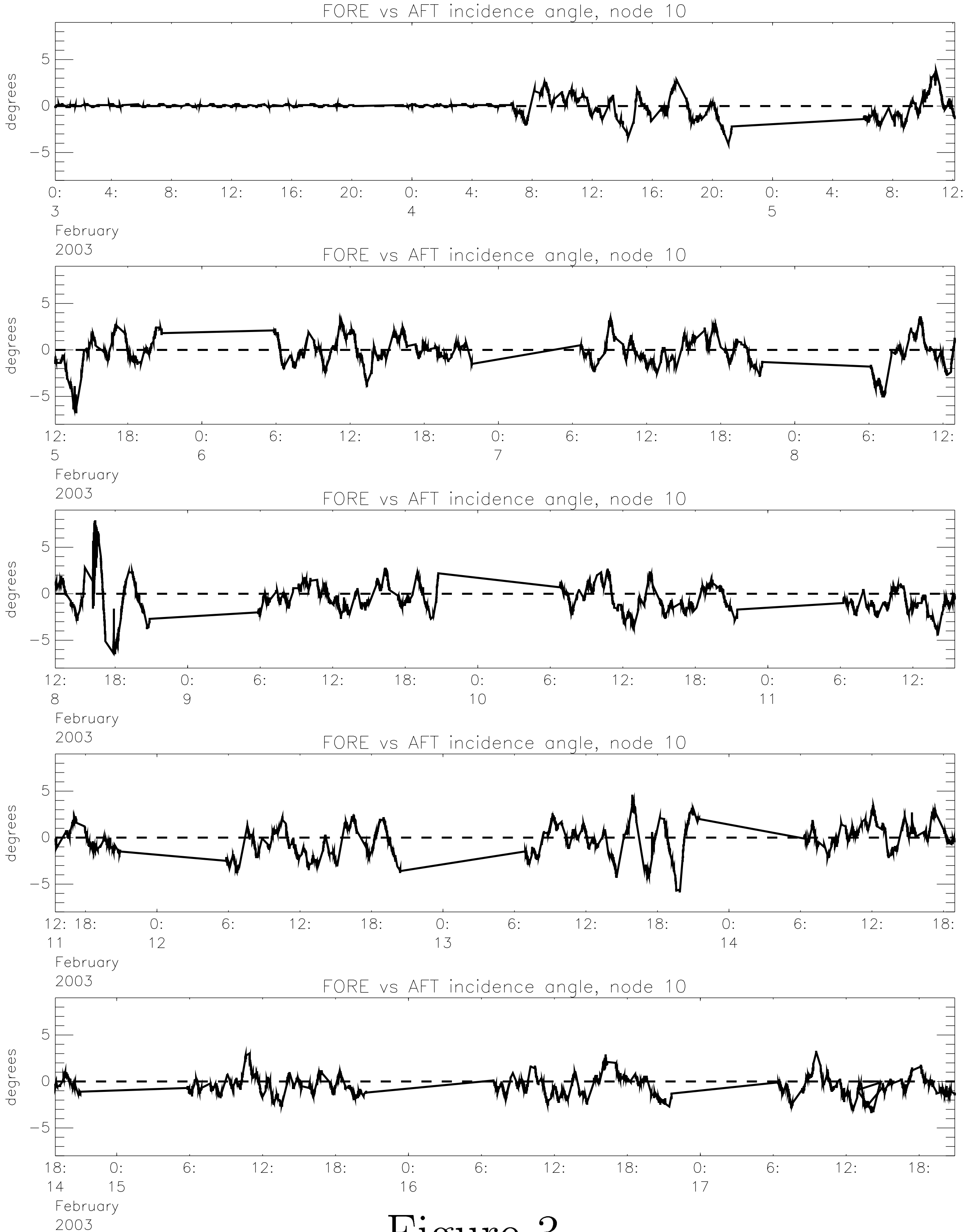
FORE vs AFT incidence angle, node 10
degrees
5
0
−5
0: 4: 8: 12: 16: 20: 0: 4: 8: 12: 16: 20: 0: 4: 8: 12:
3 4 5
February
2003
FORE vs AFT incidence angle, node 10
12: 18: 0: 6: 12: 18: 0: 6: 12: 18: 0: 6: 12:
5 6 7 8
February
2003
FORE vs AFT incidence angle, node 10
12: 18: 0: 6: 12: 18: 0: 6: 12: 18: 0: 6: 12:
8 9 10 11
February
2003
FORE vs AFT incidence angle, node 10
12: 18: 0: 6: 12: 18: 0: 6: 12: 18: 0: 6: 12: 18:
11 12 13 14
February
2003
FORE vs AFT incidence angle, node 10
18: 0: 6: 12: 18: 0: 6: 12: 18: 0: 6: 12: 18:
14 15 16 17
February
2003

Figure 3

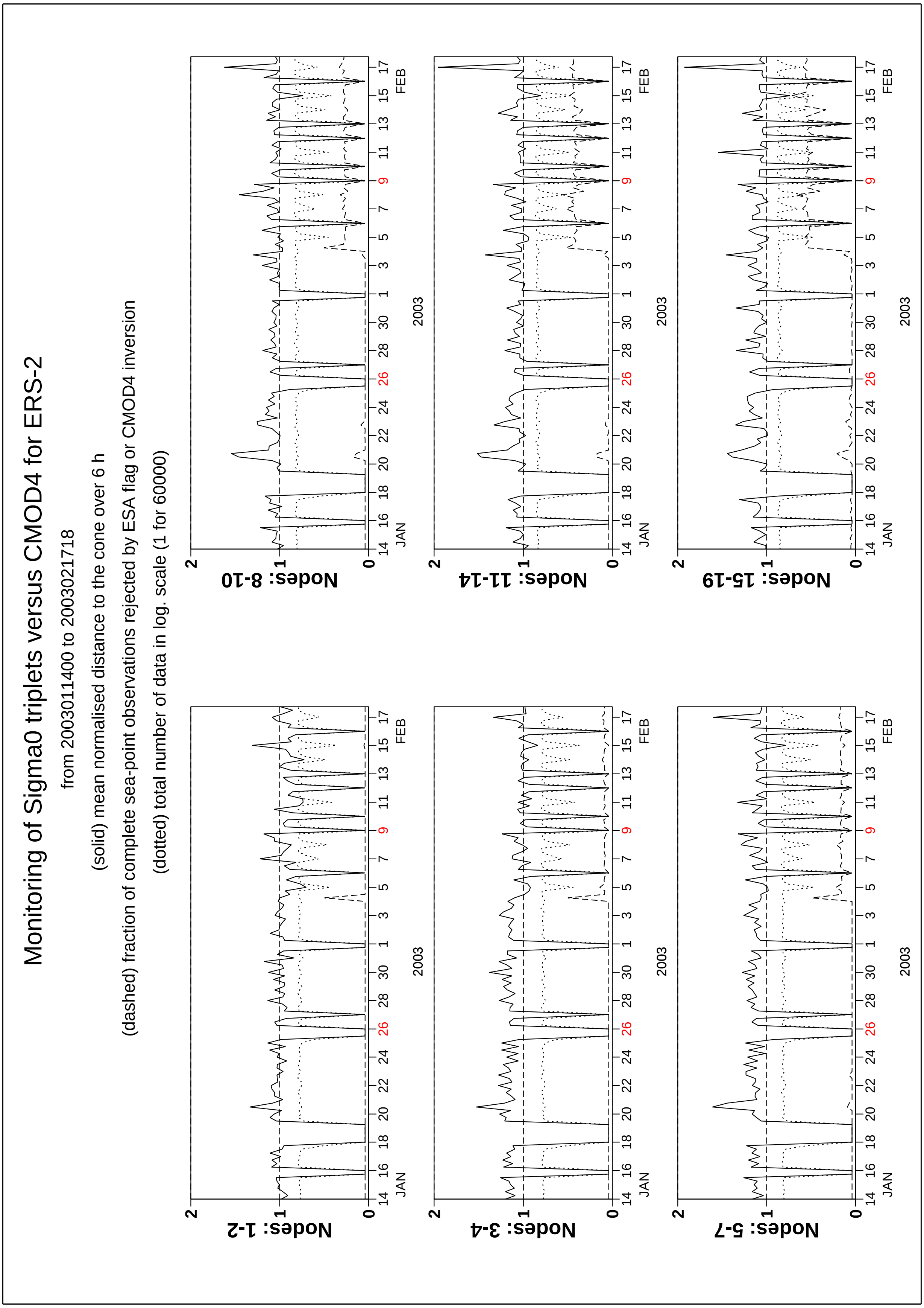
Monitoring of Sigma0 triplets versus CMOD4 for ERS-2
from 2003011400 to 2003021718
(solid) mean normalised distance to the cone over 6 h
(dashed) fraction of complete sea-point observations rejected by ESA flag or CMOD4 inversion
(dotted) total number of data in log. scale (1 for 60000)
Nodes: 1-2
Nodes: 3-4
Nodes: 5-7
Nodes: 8-10
Nodes: 11-14
Nodes: 15-19
JAN
FEB
2003

Figure 4

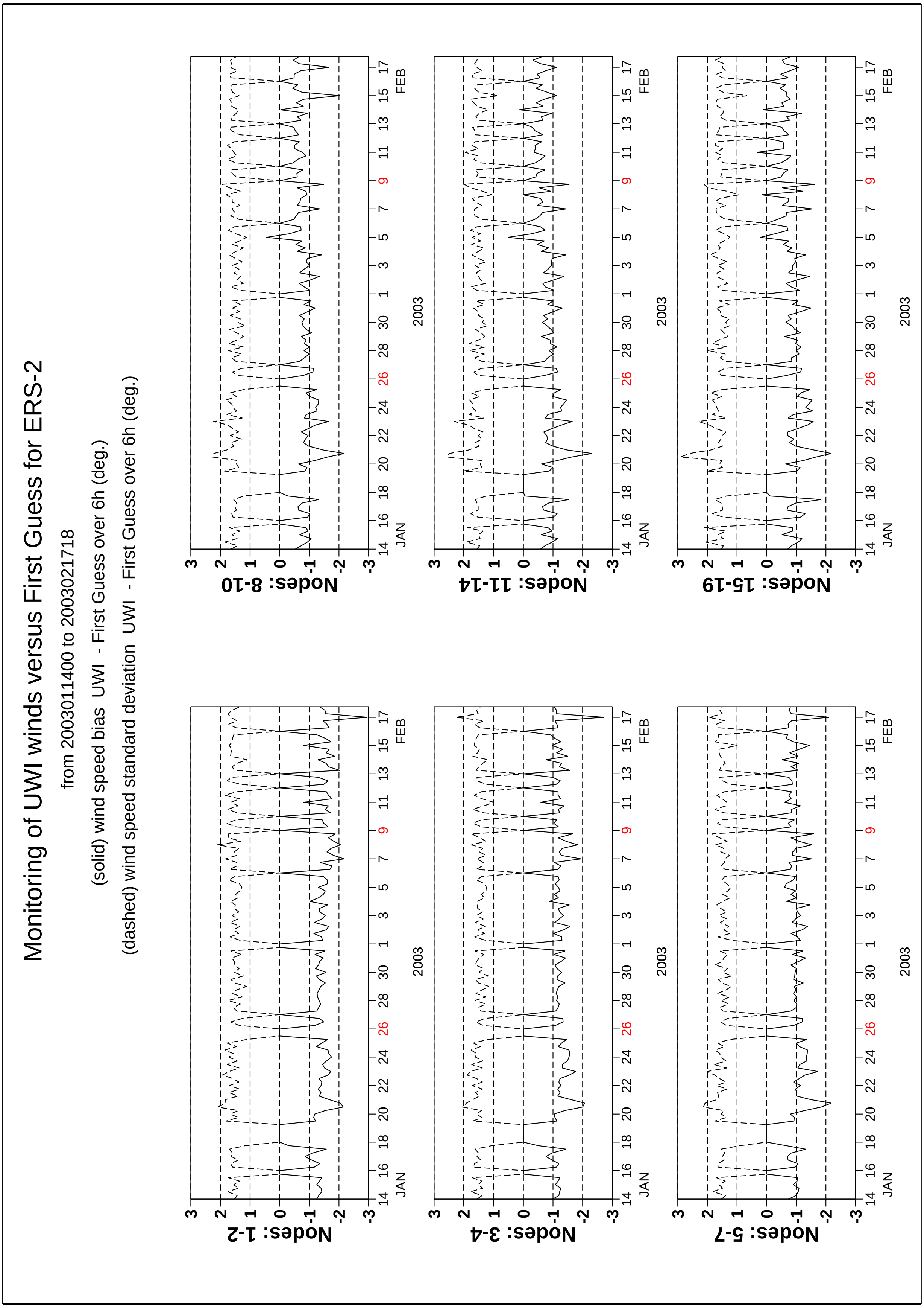
Monitoring of UWI winds versus First Guess for ERS-2
from 2003011400 to 2003021718
(solid) wind speed bias UWI - First Guess over 6h (deg.)
(dashed) wind speed standard deviation UWI - First Guess over 6h (deg.)
Nodes: 1-2
Nodes: 3-4
Nodes: 5-7
Nodes: 8-10
Nodes: 11-14
Nodes: 15-19
JAN
FEB
2003

Figure 5

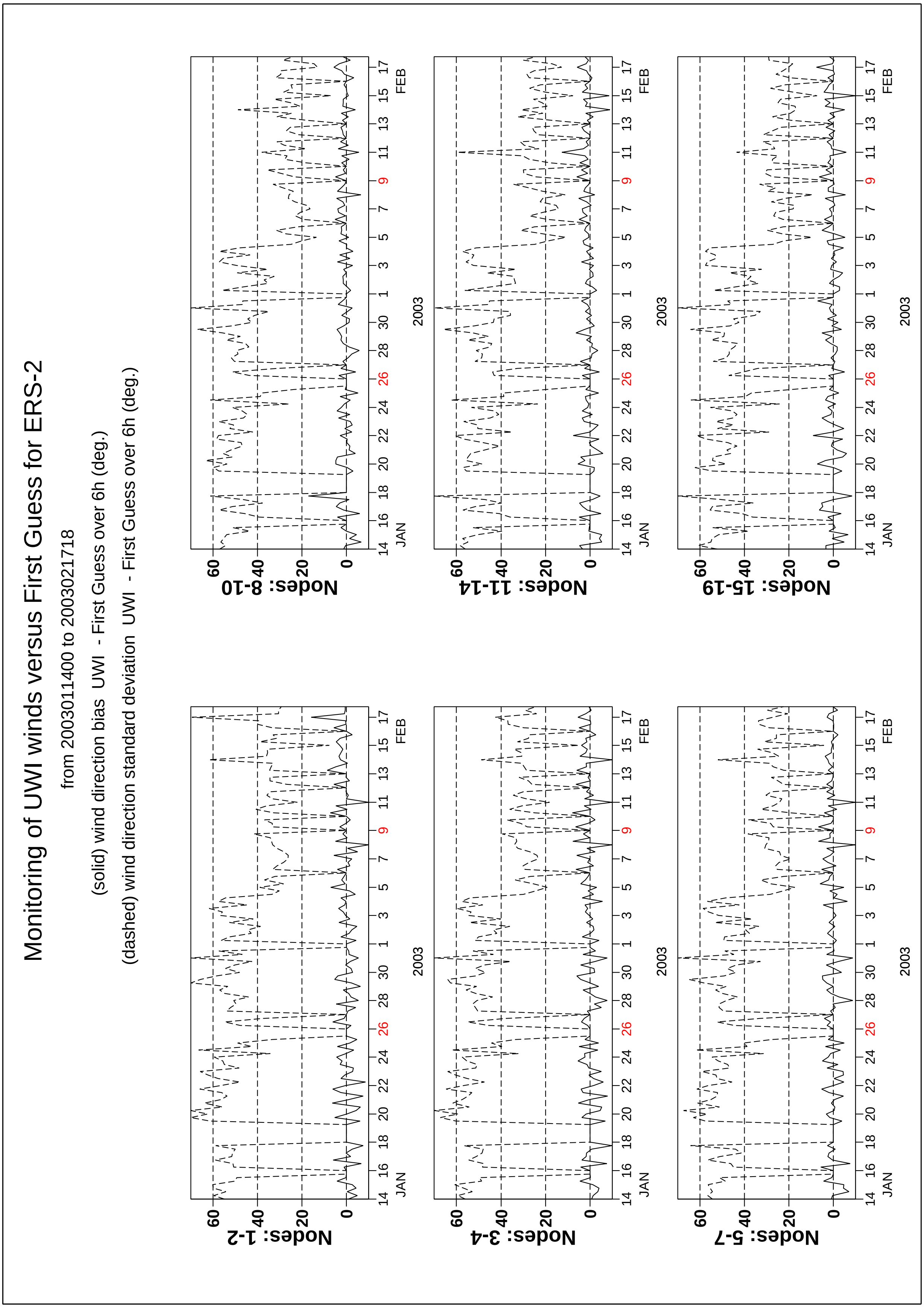
Monitoring of UWI winds versus First Guess for ERS-2
from 2003011400 to 2003021718
(solid) wind direction bias UWI - First Guess over 6h (deg.)
(dashed) wind direction standard deviation UWI - First Guess over 6h (deg.)
Nodes: 1-2
Nodes: 3-4
Nodes: 5-7
Nodes: 8-10
Nodes: 11-14
Nodes: 15-19
JAN
FEB
2003

Figure 6

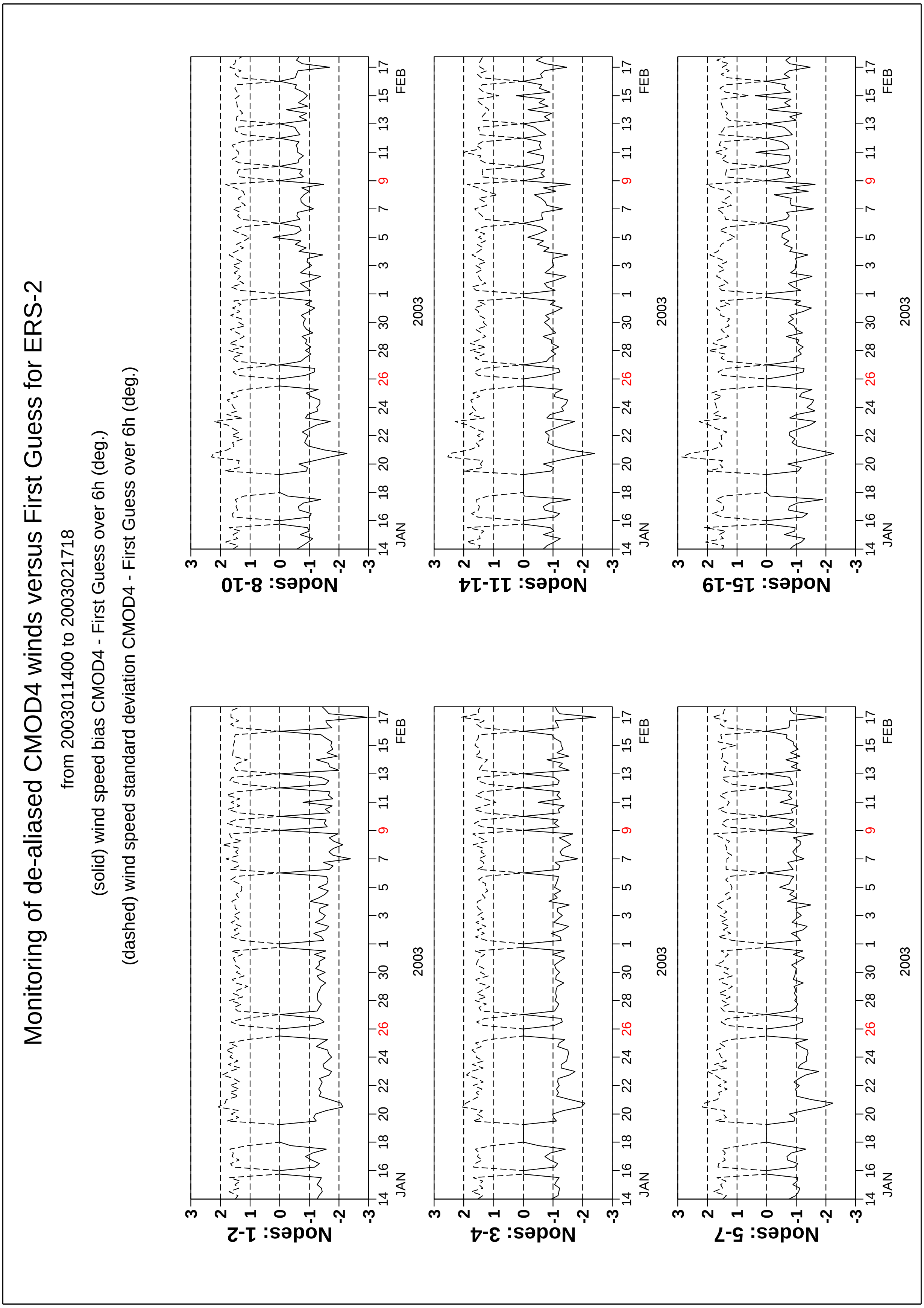
Monitoring of de-aliased CMOD4 winds versus First Guess for ERS-2
from 2003011400 to 2003021718
(solid) wind speed bias CMOD4 - First Guess over 6h (deg.)
(dashed) wind speed standard deviation CMOD4 - First Guess over 6h (deg.)
Nodes: 1-2
Nodes: 3-4
Nodes: 5-7
Nodes: 8-10
Nodes: 11-14
Nodes: 15-19
JAN
FEB
2003

Figure 7

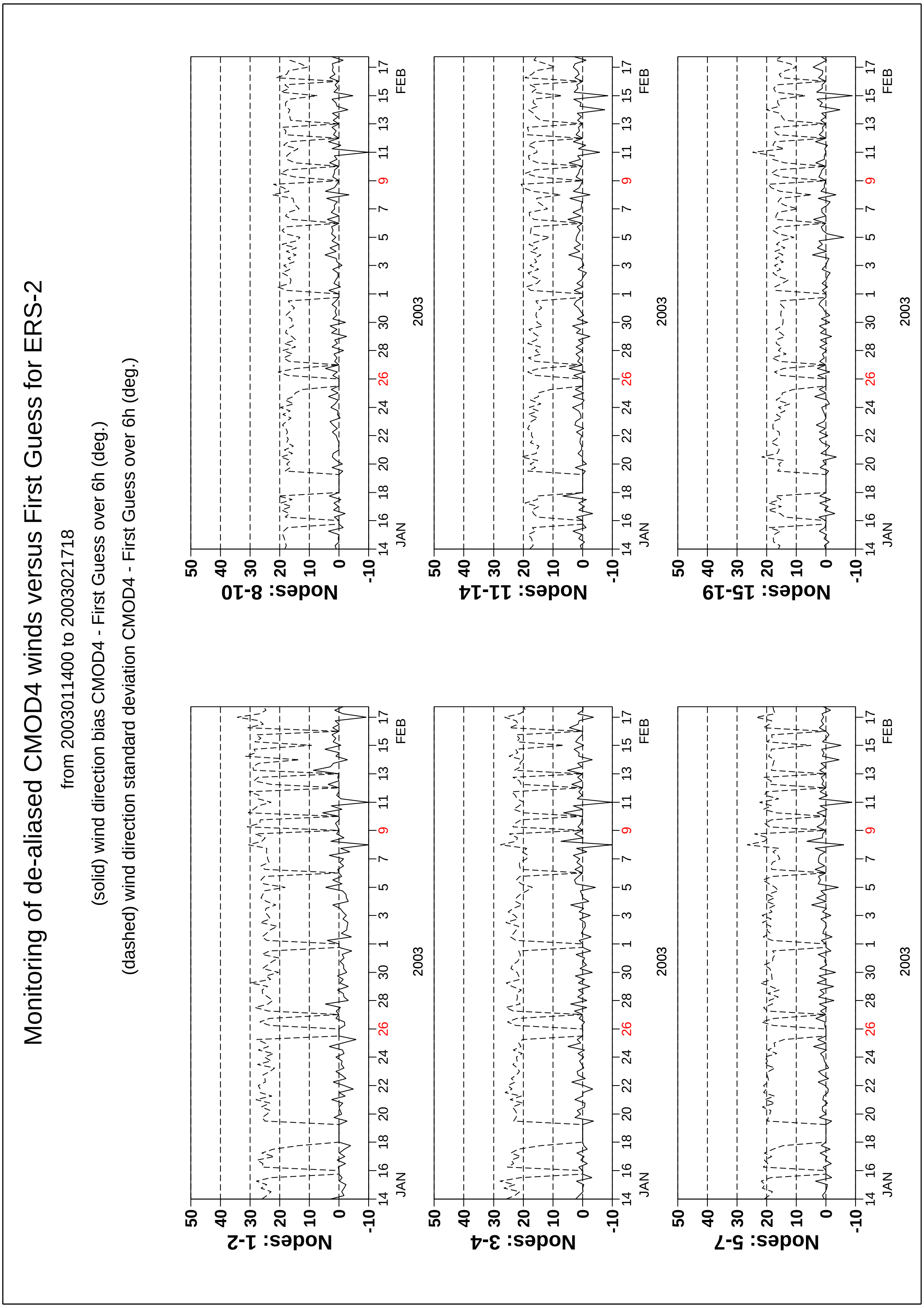
Monitoring of de-aliased CMOD4 winds versus First Guess for ERS-2
from 2003011400 to 2003021718
(solid) wind direction bias CMOD4 - First Guess over 6h (deg.)
(dashed) wind direction standard deviation CMOD4 - First Guess over 6h (deg.)
Nodes: 1-2
Nodes: 3-4
Nodes: 5-7
Nodes: 8-10
Nodes: 11-14
Nodes: 15-19
JAN
FEB
2003

Figure 8

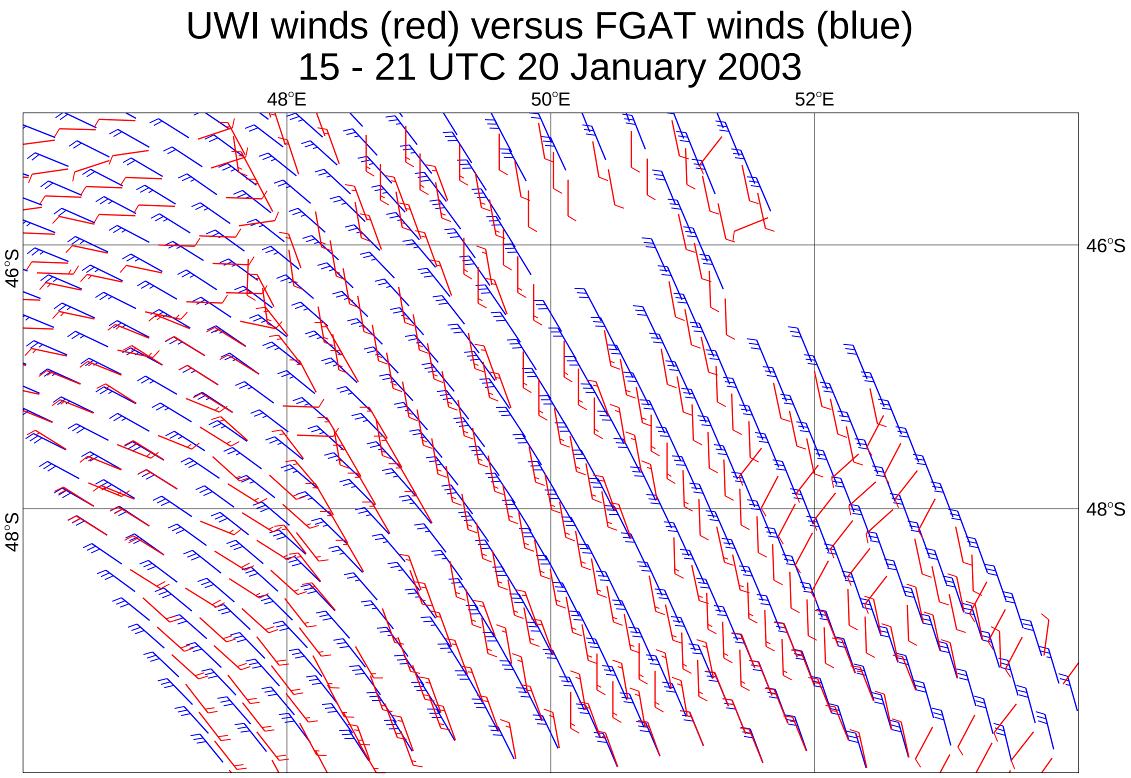
UWI winds (red) versus FGAT winds (blue)
15 - 21 UTC 20 January 2003
48°E
50°E
52°E
46°S
48°S

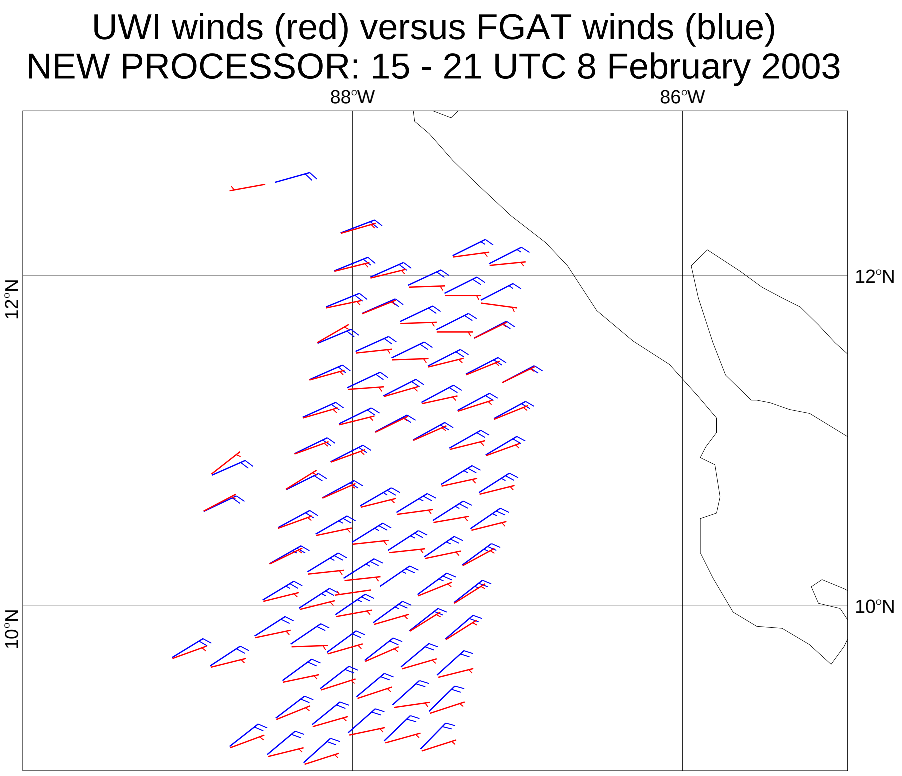
UWI winds (red) versus FGAT winds (blue)
NEW PROCESSOR: 15 - 21 UTC 8 February 2003
88°W
86°W
12°N
10°N

Figure 9

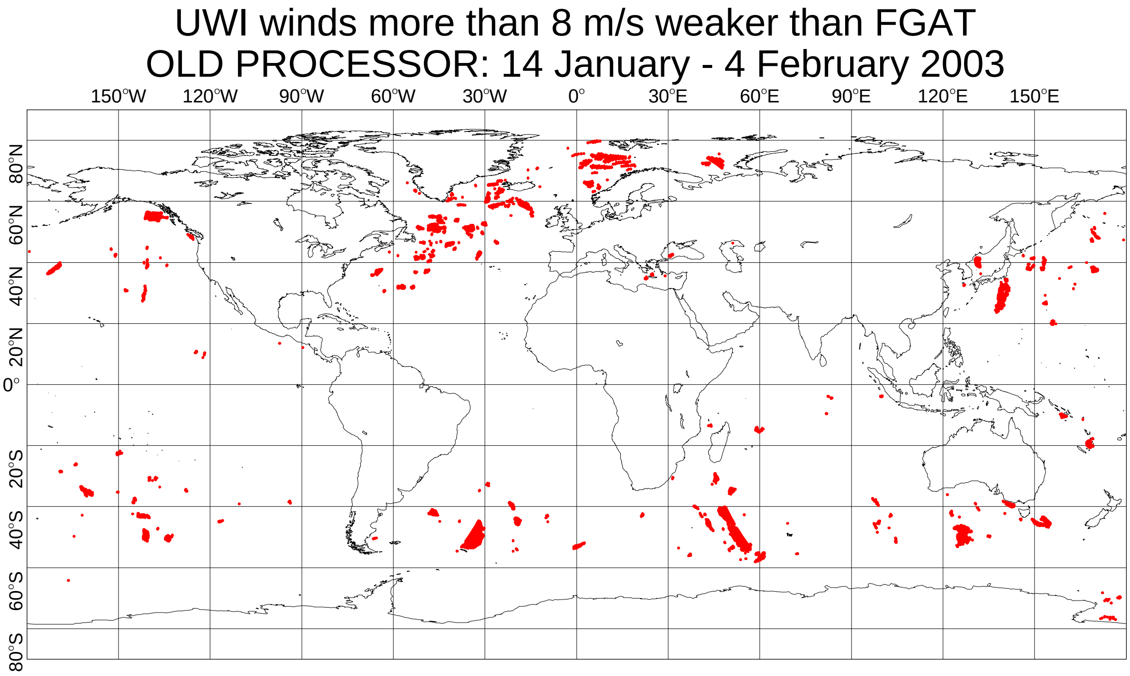
UWI winds more than 8 m/s weaker than FGAT
OLD PROCESSOR: 14 January - 4 February 2003
150°W
120°W
90°W
60°W
30°W
0°
30°E
60°E
90°E
120°E
150°E
80°N
60°N
40°N
20°N
0°
20°S
40°S
60°S
80°S

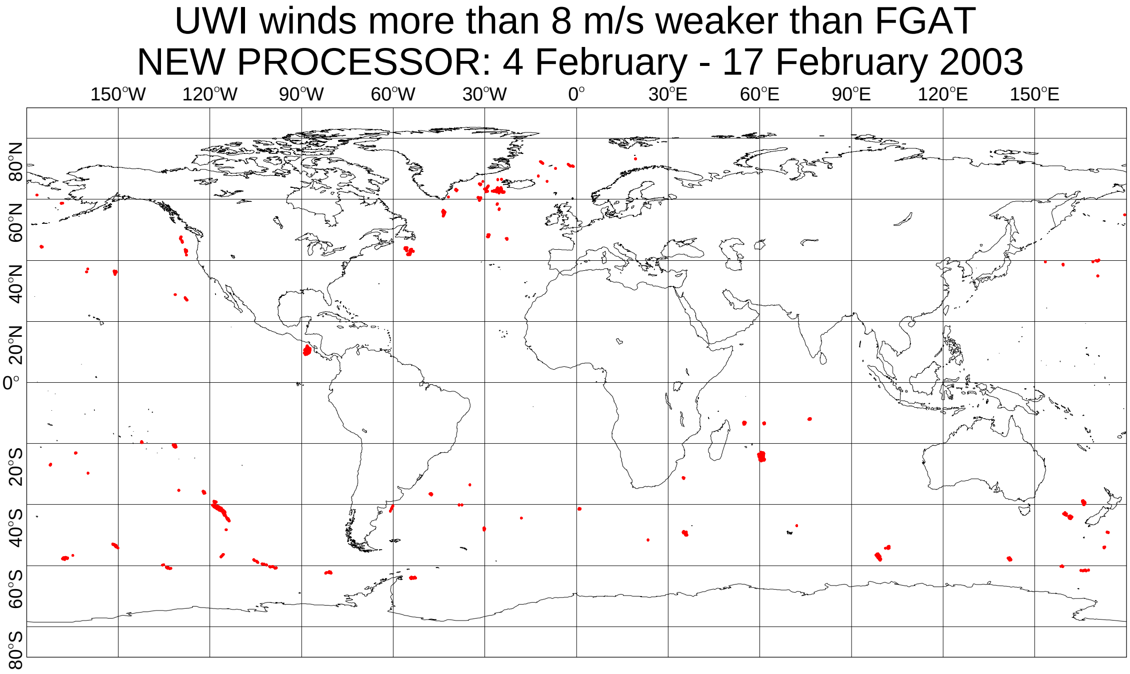
UWI winds more than 8 m/s weaker than FGAT
NEW PROCESSOR: 4 February - 17 February 2003
150°W
120°W
90°W
60°W
30°W
0°
30°E
60°E
90°E
120°E
150°E
80°N
60°N
40°N
20°N
0°
20°S
40°S
60°S
80°S

Figure 10

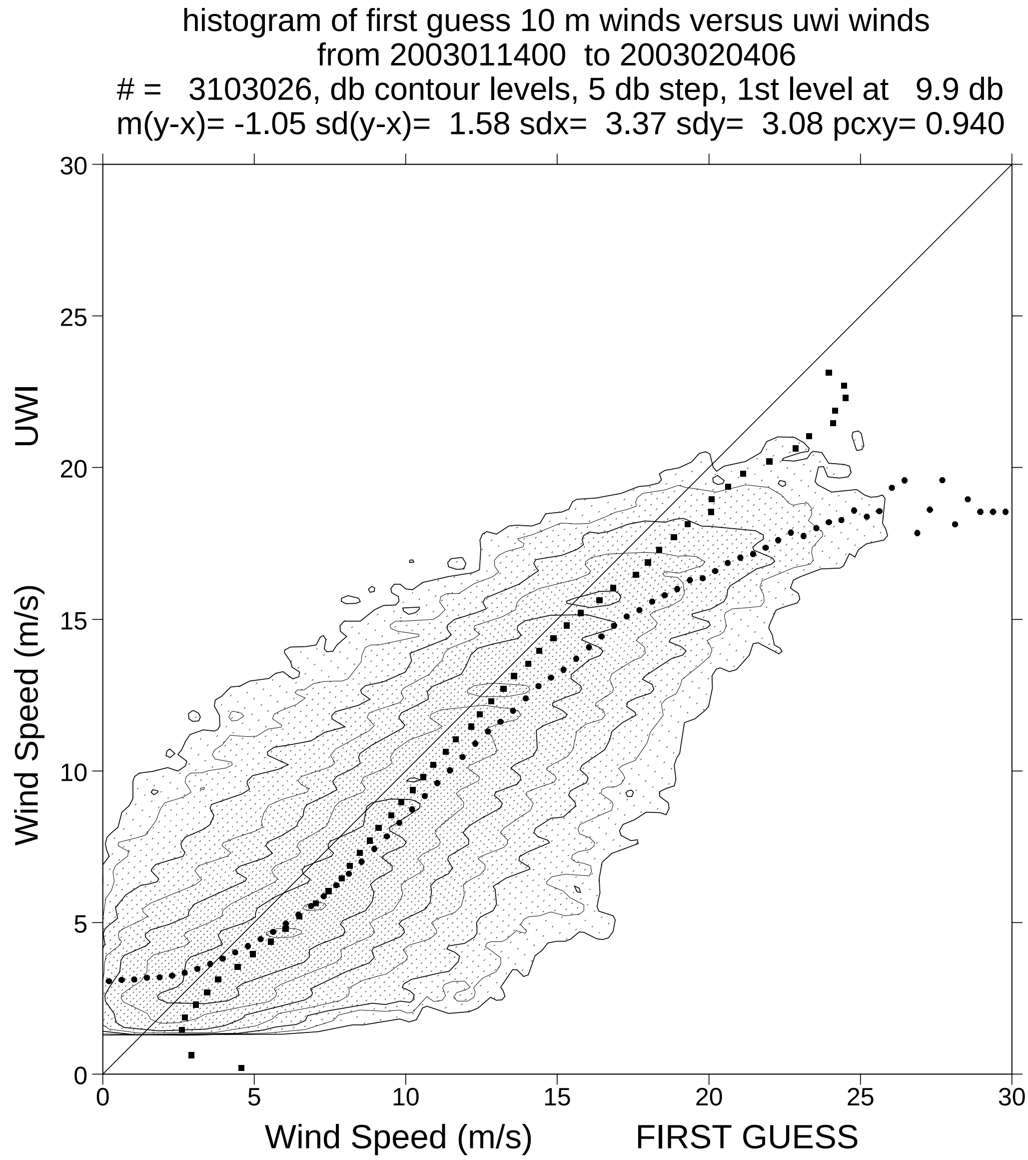
histogram of first guess 10 m winds versus uwi winds
from 2003011400 to 2003020406
= 3103026, db contour levels, 5 db step, 1st level at 9.9 db
m(y-x)= -1.05 sd(y-x)= 1.58 sdx= 3.37 sdy= 3.08 pcxy= 0.940
UWI
Wind Speed (m/s)
Wind Speed (m/s)
FIRST GUESS
0
5
10
15
20
25
30

Figure 11

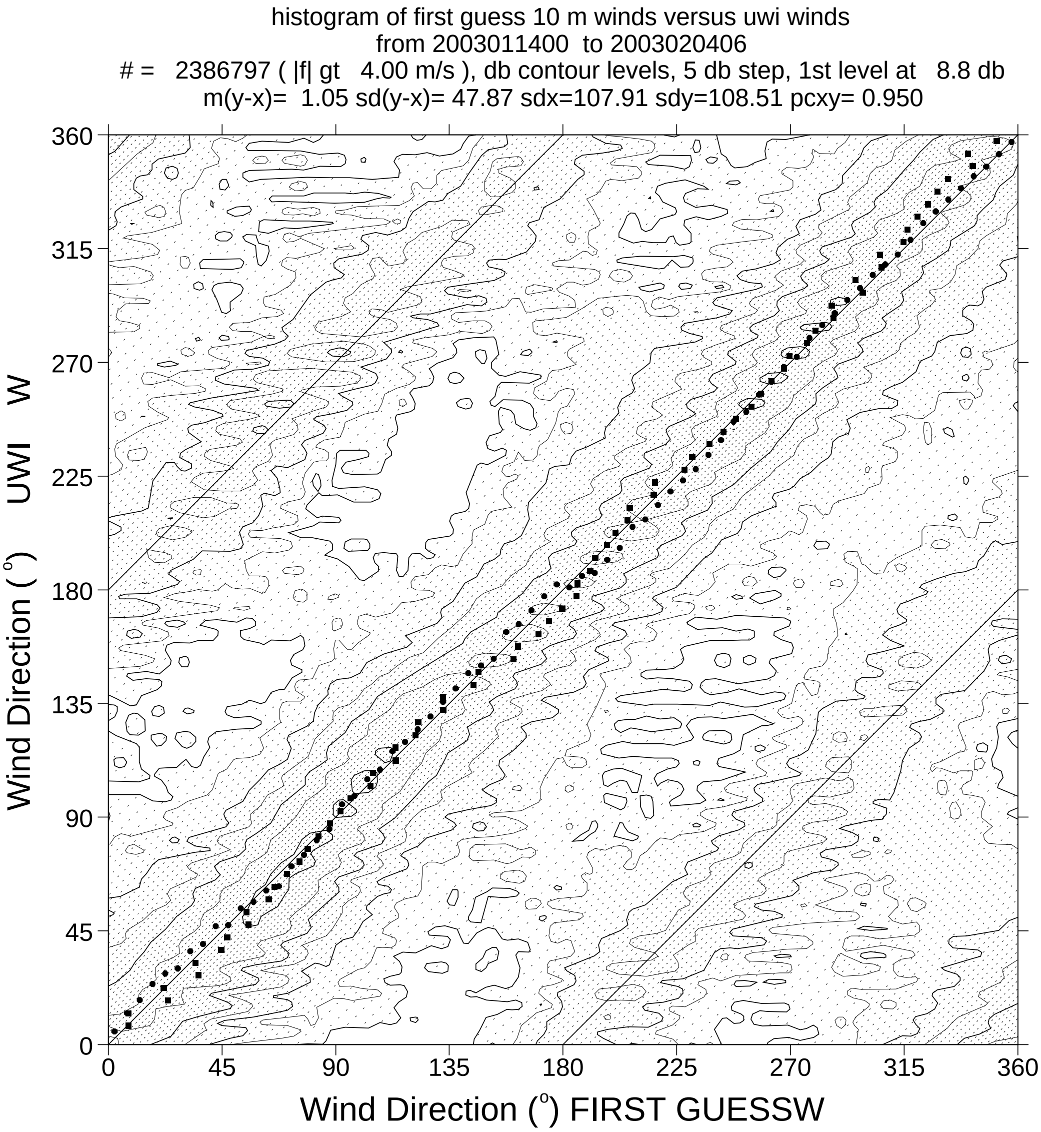
histogram of first guess 10 m winds versus uwi winds
from 2003011400 to 2003020406
= 2386797 (|f| gt 4.00 m/s), db contour levels, 5 db step, 1st level at 8.8 db
m(y-x)= 1.05 sd(y-x)= 47.87 sdx=107.91 sdy=108.51 pcxy= 0.950
Wind Direction (o) UWI W
Wind Direction (o) FIRST GUESSW
0
45
90
135
180
225
270
315
360

Figure 12

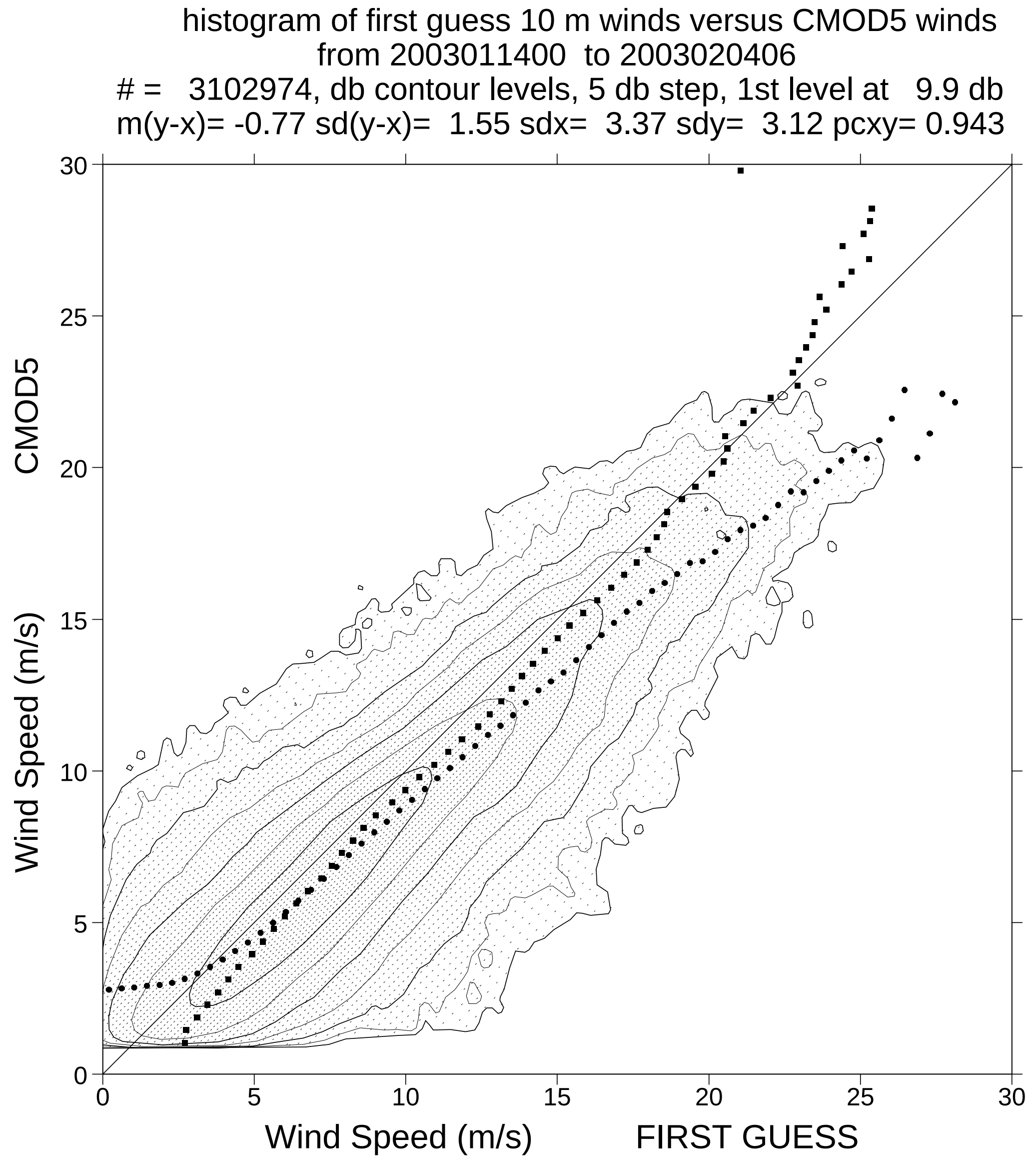
histogram of first guess 10 m winds versus CMOD5 winds
from 2003011400 to 2003020406
= 3102974, db contour levels, 5 db step, 1st level at 9.9 db
m(y-x)= -0.77 sd(y-x)= 1.55 sdx= 3.37 sdy= 3.12 pcxy= 0.943
CMOD5
Wind Speed (m/s)
Wind Speed (m/s)
FIRST GUESS
0
5
10
15
20
25
30

Figure 13

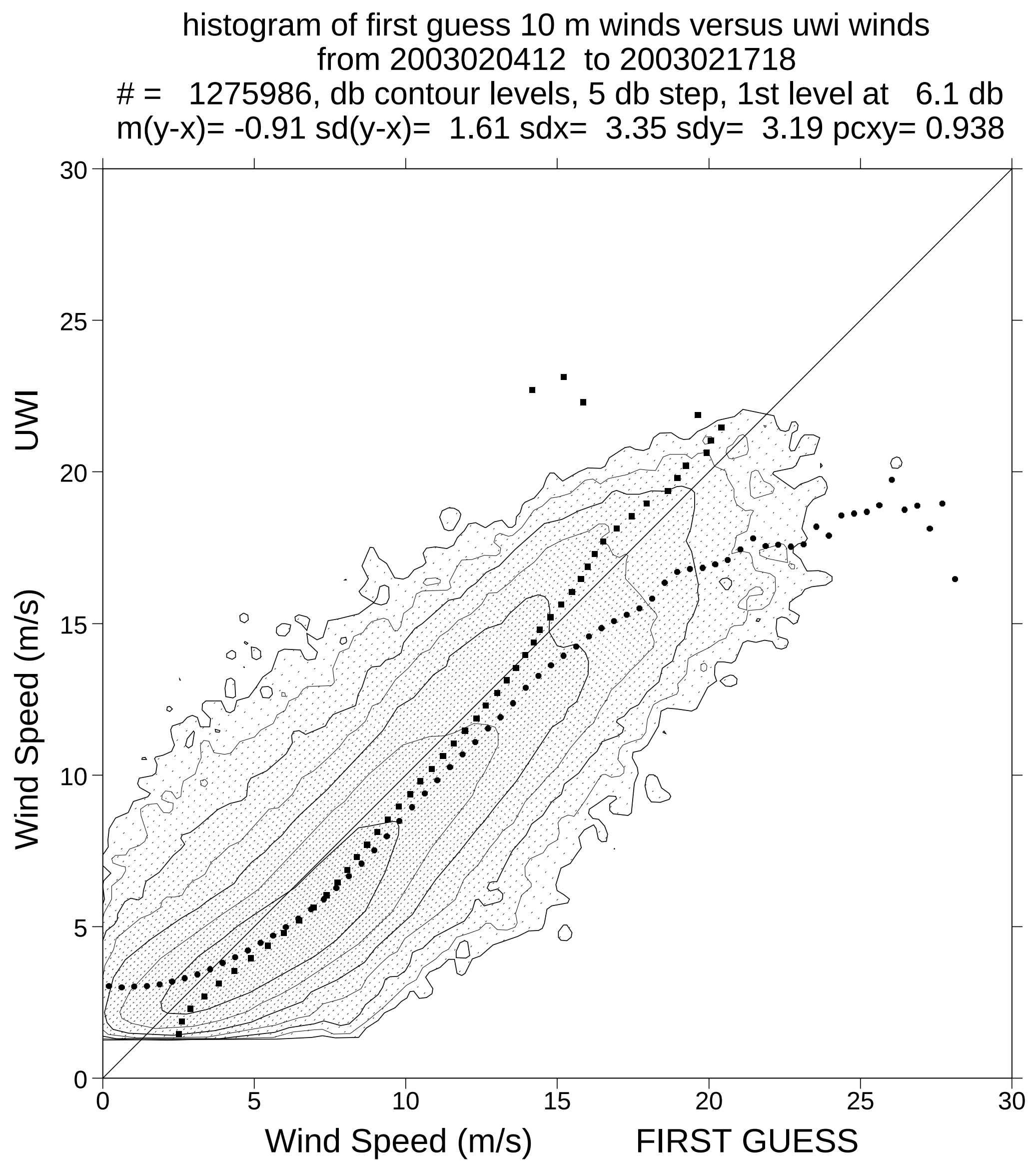
histogram of first guess 10 m winds versus uwi winds
from 2003020412 to 2003021718
= 1275986, db contour levels, 5 db step, 1st level at 6.1 db
m(y-x)= -0.91 sd(y-x)= 1.61 sdx= 3.35 sdy= 3.19 pcxy= 0.938
UWI
Wind Speed (m/s)
0
5
10
15
20
25
30
0
5
10
15
20
25
30
Wind Speed (m/s)
FIRST GUESS

Figure 14

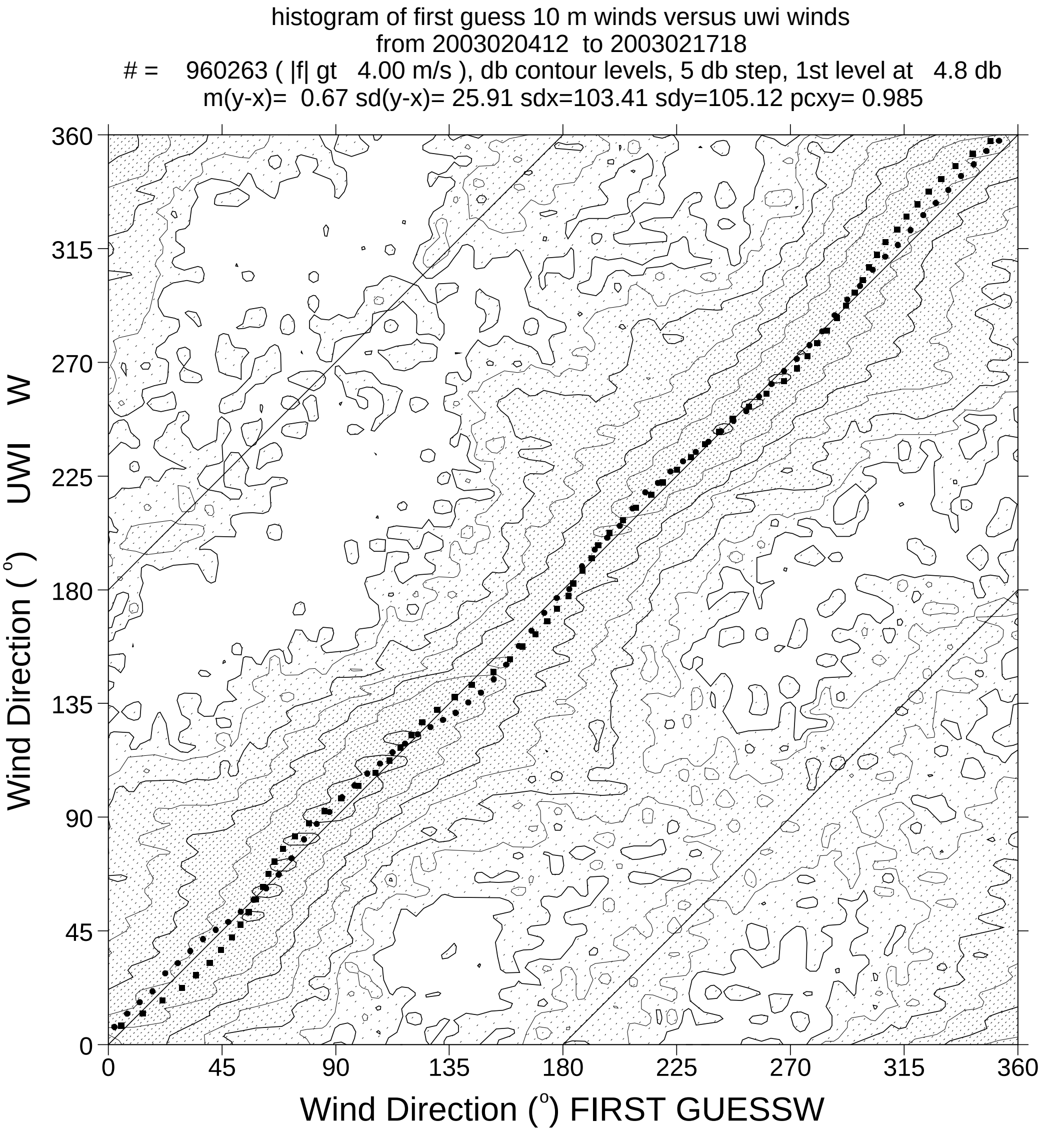
histogram of first guess 10 m winds versus uwi winds
from 2003020412 to 2003021718
= 960263 (|f| gt 4.00 m/s), db contour levels, 5 db step, 1st level at 4.8 db
m(y-x)= 0.67 sd(y-x)= 25.91 sdx=103.41 sdy=105.12 pcxy= 0.985
Wind Direction (o) UWI W
Wind Direction (o) FIRST GUESSW
0
45
90
135
180
225
270
315
360

Figure 15

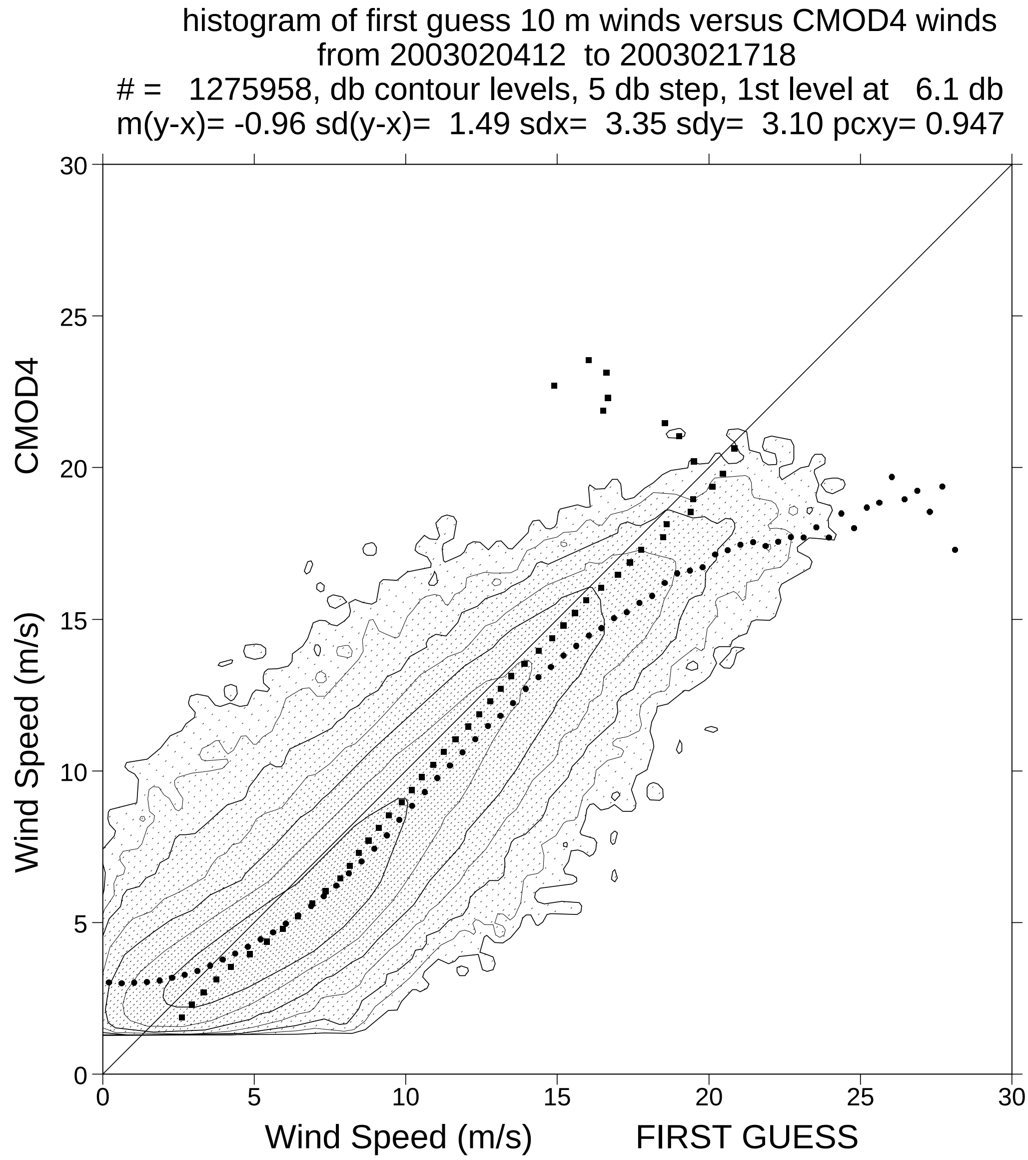

histogram of first guess 10 m winds versus CMOD4 winds
from 2003020412 to 2003021718
= 1275958, db contour levels, 5 db step, 1st level at 6.1 db
m(y-x)= -0.96 sd(y-x)= 1.49 sdx= 3.35 sdy= 3.10 pcxy= 0.947
CMOD4
Wind Speed (m/s)
Wind Speed (m/s)
FIRST GUESS
0
5
10
15
20
25
30

Figure 16

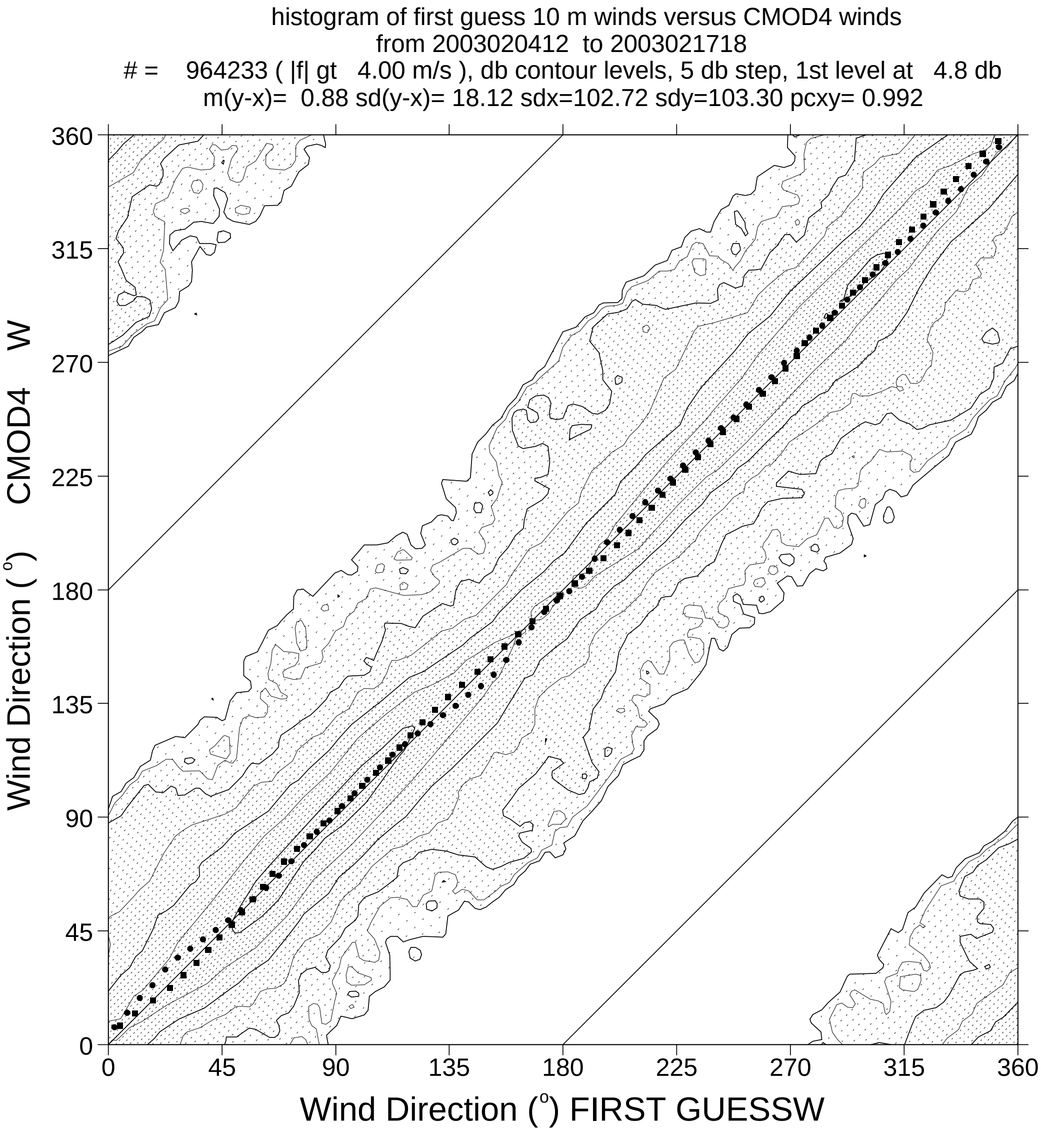
histogram of first guess 10 m winds versus CMOD4 winds
from 2003020412 to 2003021718
= 964233 (|f| gt 4.00 m/s), db contour levels, 5 db step, 1st level at 4.8 db
m(y-x)= 0.88 sd(y-x)= 18.12 sdx=102.72 sdy=103.30 pcxy= 0.992
Wind Direction (°) CMOD4 W
Wind Direction (°) FIRST GUESSW
0
45
90
135
180
225
270
315
360

Figure 17

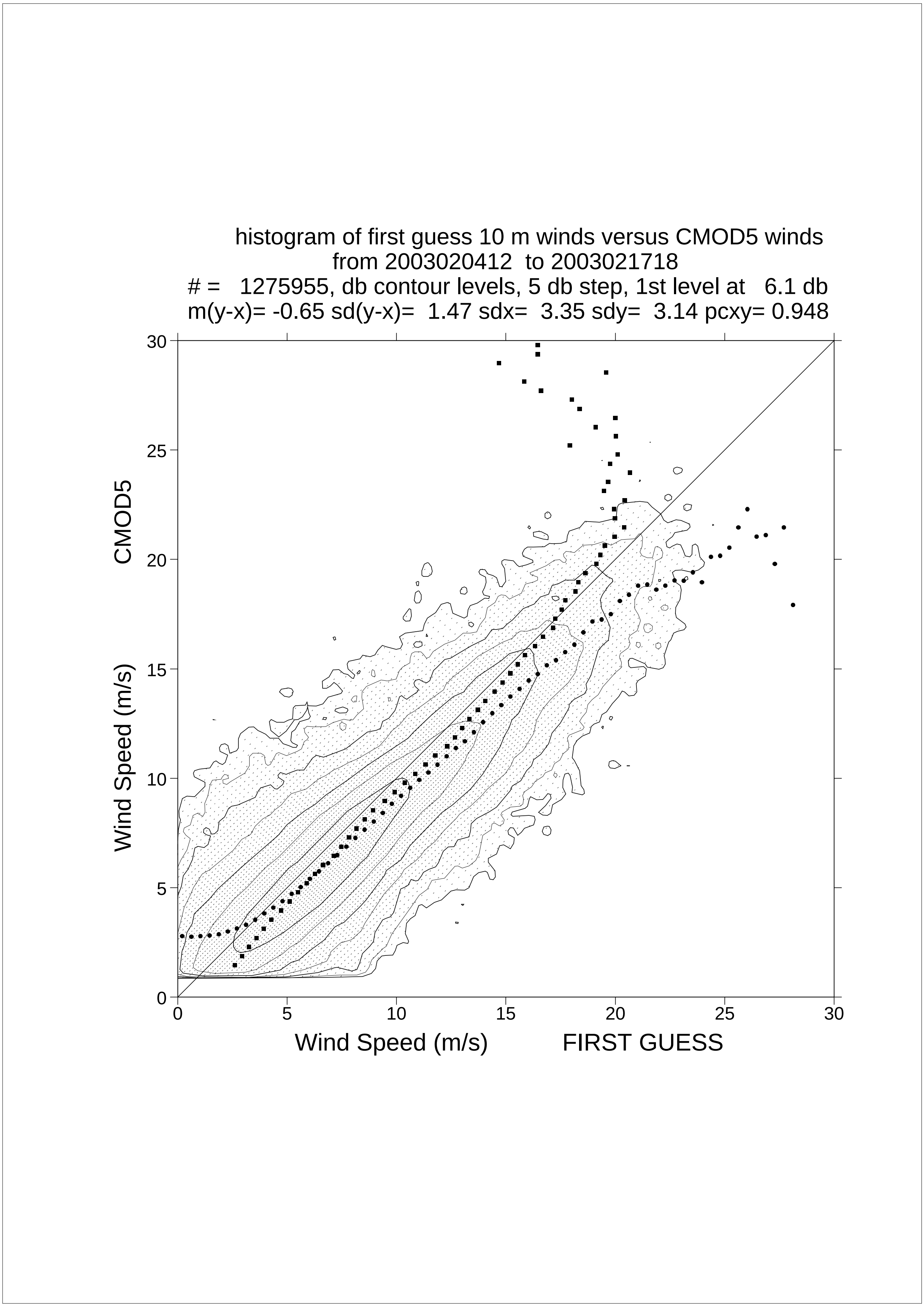
histogram of first guess 10 m winds versus CMOD5 winds
from 2003020412 to 2003021718
= 1275955, db contour levels, 5 db step, 1st level at 6.1 db
m(y-x)= -0.65 sd(y-x)= 1.47 sdx= 3.35 sdy= 3.14 pcxy= 0.948
CMOD5
Wind Speed (m/s)
Wind Speed (m/s)
FIRST GUESS
0
5
10
15
20
25
30

Figure 18